fMRI based fiber tracking using SENSE-DTI at 3 Tesla

P. Staempfli[1,2], T. Jaermann[1,2], A. Valavanis[2], P. Boesiger[1], S. S. Kollias[2]

[1]Institute for Biomedical Engineering, ETH and University Zurich, Zurich, Switzerland, [2]Institute of Neuroradiology, University Hospital Zurich, Zurich, Switzerland

Introduction

At present, Diffusion Tensor Imaging (DTI) is the only non-invasive imaging method for studying the anatomy of white matter structure in the human brain *in-vivo*. Fiber tracking algorithms make it possible to reconstruct the three-dimensional architecture of the major white matter tracts within the living human brain (for a review, see [1]). One of the topics which is currently receiving increasing attention are new functional MRI (fMRI)-based tracking methods. A previous study [2] showed a possible clinical application which combines information on the functional cortical organization provided by fMRI with anatomical information on cerebral myeloarchitectonics provided by DTI. In this work, we explore the use of fMRI-evoked DT tracking using sensitivity encoded (SENSE) [3] data acquired at 3 Tesla. Tracking algorithms are sensitive to errors in regions where the diffusion tensor does not have a strong directional component due to fiber crossing or bifurcation. To overcome this problem, a DTI/fMRI tracking algorithm based on the tensor deflection method (TEND) [4] was implemented.

Methods

Data were obtained by applying the new tracking algorithm to volunteer and patient DTI- and fMRI studies acquired at a 3 Tesla MR system with strong gradients using SENSE. DTI and fMRI data were acquired from three healthy volunteers, two patients suffering from arteriovenous malformation (AVM) and one tumor patient, using a 3-T Philips Intera whole body system (Philips Medical Systems, Best, the Netherlands) equipped with 80 mT/m, 200 mT/m/ms gradient coils and a 8-element receive head coil array (MRI Devices Corp., Waukesha, USA). For the DTI data, a SENSE reduction factor R =2.1 was used in a single-shot SE-EPI scheme (matrix = 96x96, *FOV* = 200x200x90mm, 36 slices, slice thickness = 2.5mm, *TE* = 74ms, *TR* = 8846ms). Diffusion weighting with a *b*-factor of 1000 s/mm^2 was carried out along six directions, complemented by one scan with $b = 0$. The fMRI experiments were performed in the same session using a single-shot GE-EPI pulse sequence with the same resolution as the DTI experiments (TE = 35ms, TR = 3000ms and $\alpha = 85^{\circ}$). The functional paradigm consisted of three periods of motor activity alternating with rest, each of them defined as follows: 10xTR on, 10xTR off. In the post-processing phase, eddy-current-induced image warping was removed from the DTI data with a 3D-registration algorithm [5] and the diffusion tensor's properties were derived by singular value decomposition. For the fiber-tracking, a new algorithm, based on the TEND method, was implemented. The DTI-images and the calculated fMRI statistical activation maps were superimposed and registered by a manual rigid transformation. The tracking was started in 3D-seed-areas (3D-SAs) (multi seed-forward-integration), which were computed automatically based on fMRI activation regions. Because fMRI activations are located mainly in gray matter where the anisotropy is low, the SAs were increased volumetric in order to start the tracking in the white matter adjacent to the activated cortex. All tracking calculations and the subsequent visualization were performed using a custom-made software component which is integrated into the 3D-visualisation-environment "Bitplane Imaris" [6].

Results

Figure 1a shows an automatically calculated 3D-SA in a volunteer dataset, based on finger-tapping fMRI-activations. In figure 1b, a 3D-SA in a dataset of an AVM patient is displayed. It was generated from a motor finger-tapping fMRI experiment. The fiber tracking results of the volunteer dataset are presented in figure 2. The tracking results performed in the AVM dataset are shown in figure 3. The fibers on the right side in figure 3 were calculated from the 3D-SA in the AVM region (figure 1b). For comparison, the fibers on the left side in figure 3 were calculated out of a manually defined 3D-SA in the motor cortex of the non AVM affected hemisphere. As compared to the normal volunteer data, the reduced activation in the primary motor cortex in the area of the AVM is also associated with a reduced number of projectional corticospinal fibers.

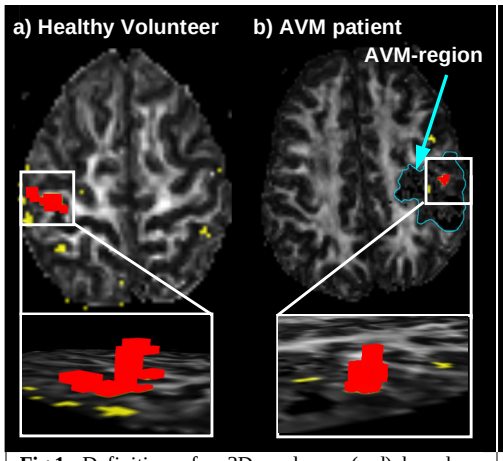

Fig.1: Definition of a 3D-seed-area (red) based on fMRI finger tapping activation areas (yellow) which are superimposed on the FA data. At the bottom of the figure, the M1 activation regions are zoomed in.
a) Dataset of a left handed healthy volunteer
b) Right handed AVM patient (AVM region is indicated by the blue arrow)

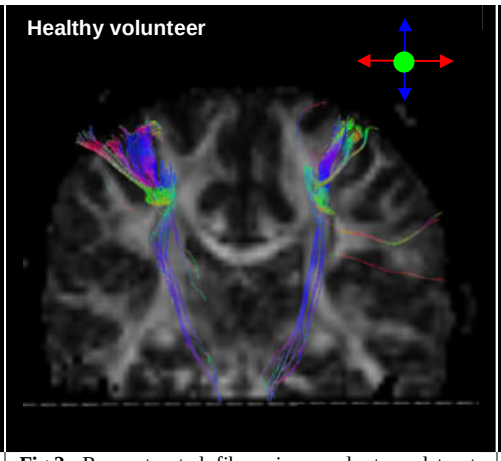

Fig.2: Reconstructed fibers in a volunteer dataset. Each color corresponds to a directional orientation as indicated on top right. On the activation side (left side in the figure), the fMRI evoked fibers are shown which were reconstructed out of the SA of figure 1a. As comparison, the fibers on contralateral side were reconstructed out of a manually defined SA in the motor cortex of the contralateral hemisphere.

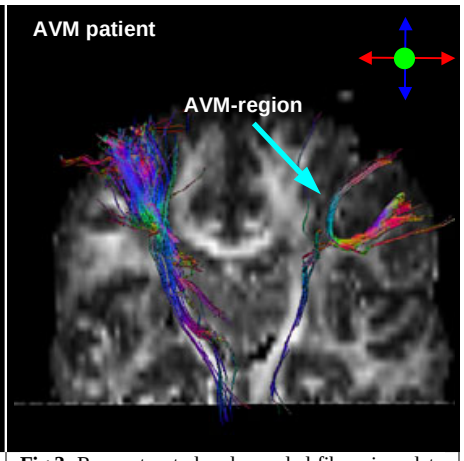

Fig.3: Reconstructed, color coded fibers in a data set of an AVM patient. The fibers on the side of the lesion (blue arrow) were reconstructed out of the fMRI region of figure 1b. As comparison, the fibers on the contralateral side were reconstructed from a manually defined ROI in the contralateral primary motor cortex.

Discussion and Conclusion

In this study we have shown that the implemented tracking algorithm improves the results in regions in which fiber crossing occurs, since not only the direction of the main eigenvector but the whole tensor information is considered. Further advances in combining fMRI and DTI data sets is a promising tool for addressing issues of functional connectivity in the human brain in vivo. In the clinical setting, this approach holds great promise for better understanding the reorganizational changes of the brain in the presence of disease, and for providing a improved information for treatment planning.

References

1. Mori S, et al NMR in Biomedicine 2002, 15: 468-480 2. Hendler T, et al. *Proc. Int Soc Magn Reson Med*: 394, 2003. 3. 3. Pruessmann KP, et.al. Magn Reson Med 1999; 42: 952-962. 4. Lazar, M, et.al. Human Brain Mapping 2003; 18: 306-321. 5. Netsch T, et.al. *Proc. ICCV*: 718-725, 2001. 6. www.bitplane.com.